

**Amino acid contacts between Sigma 70 domain 4 and the
transcription activators RhaS and RhaR**

Running Title: RhaS and RhaR amino acid contacts with σ^{70} domain 4

Jason R. Wickstrum and Susan M. Egan*

**Department of Molecular Biosciences
University of Kansas, Lawrence, KS 66045**

***Corresponding author: email: sme@ku.edu**

ABSTRACT

The RhaS and RhaR proteins are transcription activators that respond to the availability of L-rhamnose and activate transcription of the operons in the *E. coli* L-rhamnose catabolic regulon. RhaR activates transcription of *rhaSR*, and RhaS activates transcription of the operon that encodes the L-rhamnose catabolic enzymes, *rhaBAD*, as well as the operon that encodes the L-rhamnose transport protein, *rhaT*. RhaS is 30% identical to RhaR at the amino acid level and both are members of the AraC/XylS family of transcription activators. The RhaS and RhaR binding sites overlap the -35 hexamers of the promoters they regulate, suggesting they may contact the σ^{70} subunit of RNA polymerase as part of their mechanisms of transcription activation. In support of this hypothesis, our lab previously identified an interaction between RhaS residue D241 and σ^{70} residue R599. Here, we first identified two positively charged amino acids in σ^{70} , K593 and R599, and three negatively charged amino acids in RhaR, D276, E284, and D285, that were important for RhaR-mediated transcription activation of the *rhaSR* operon. Using a genetic loss-of-contact approach we have obtained evidence for a specific contact between RhaR D276 and σ^{70} R599. Finally, previous results from our lab separately showed that RhaS D250A and σ^{70} K593A were defective at the *rhaBAD* promoter. Our genetic loss-of-contact analysis of these residues indicates that they identify a second site of contact between RhaS and σ^{70} .

INTRODUCTION

Transcription activation in *Escherichia coli* often involves the interaction of a DNA-binding activator protein with one of the subunits of RNA polymerase (RNAP), most often the sigma (σ) or alpha (α) subunit. Transcription activators that bind immediately upstream and adjacent to RNAP, in some cases overlapping the -35 promoter hexamer, may interact with the C-terminal domain (domain 4) of the α subunit of RNAP (8, 27). The cI protein of bacteriophage λ is required for the establishment and maintenance of lysogeny and is perhaps the best-characterized example of a transcription activator that contacts σ^{70} . The λ cI protein activates transcription of the P_{RM} promoter when bound at the O_{R2} operator site, which overlaps the P_{RM} -35 hexamer by 2 bp (30). Current evidence suggests that σ^{70} residues R588, K593, and R596 are required for activation by λ cI (23, 26, 35). Genetic and molecular modeling studies as well as the recent structure of a ternary λ cI/ α domain 4/DNA complex indicate that λ cI D38 contacts both σ^{70} K593 (α^A K418) and R596 (α^A R421), and λ cI E34 contacts σ^{70} R588 (α^A R413) (8, 19, 26, 35). Prior to the ternary complex structure, a molecular model of the interaction indicated that σ^{70} K593 (α^A K418) contacts DNA but was not positioned to contact λ cI (6, 8, 35). However, the ternary structure showed that the α^A residue that aligns with σ^{70} K593 has moved away from the DNA (relative to the model of the interaction) and instead makes a protein-protein contact with λ cI D38 (19).

There is also evidence that activation by several transcription activators in the AraC/XylS family involves σ^{70} domain 4. Our lab previously identified two σ^{70} residues, K593 and R599, which are required for full activation by RhaS, and further obtained genetic evidence that σ^{70} R599 is directly involved in a contact with RhaS D241 (4). These genetic results are also strongly supported by molecular modeling of the RhaS- σ^{70} complex on DNA (4). Evidence for AraC interactions with σ^{70} come from early σ^{70} mutants (eventually identified at R596) that increased *araBAD* expression in the absence of activation by CRP (18, 39, 44) as well as the finding that *araBAD* expression

in a \square_{cya} strain was increased by \square^{70} E591A and R596A and decreased by \square^{70} K593A (27). In addition, with a DNA that mimicked an open complex, a small amount of DNA binding cooperativity could be detected between AraC and \square^{70} (7). At the *melAB* promoter, genetic evidence indicated that \square^{70} R596 interacts with MelR D261 and T265 while \square^{70} R599 also interacts with MelR D261, which aligns with RhaS D241 (16). The Ada protein has two activation domains, one of which is an AraC/XylS family domain which is required to activate transcription of the *alkA* operon (33). Alanine substitutions of \square^{70} residues K593, K597 and R603 each had significant defects in Ada-dependent *alkA* transcription *in vivo* and *in vitro* (24).

The transcription activator RhaS, and the closely related RhaR protein, activate transcription of the *E. coli* L-rhamnose catabolic operons in the presence of the sugar L-rhamnose (10, 11, 42). RhaS activates transcription of the *rhaBAD* and *rhaT* operons by binding as a dimer to sites that overlap the -35 hexamers of the promoters by four base pairs and extend upstream to -81 and -82 , respectively (Fig. 1 for *rhaBAD* promoter) (10, 45). Similarly, RhaR activates transcription of the *rhaSR* operon by binding as a dimer to a site that overlaps the RNAP binding site by four base pairs and extends upstream to -82 (Fig. 1) (43). The long binding sites for RhaS and RhaR each consist of two 17 base pair imperfect inverted repeat half sites that are separated by 16 or 17 base pairs of uncontacted DNA (10, 43, 45). Each RhaS and RhaR monomer is predicted to contain two helix-turn-helix DNA binding motifs and thereby contact two consecutive major grooves of DNA (38). The cyclic AMP receptor protein (CRP) also activates transcription at all three of the *rha* promoters. At the *rhaBAD* and *rhaT* promoters, the CRP binding site is located immediately upstream of the RhaS binding site and is centered at -92.5 and -93.5 , respectively (Fig. 1 for *rhaBAD* promoter) (11, 45). The CRP site required for full activation at *rhaSR* is located upstream but not adjacent to the RhaR binding site and is centered at -111.5 (Fig. 1) (17).

RhaS and RhaR are members of a subset of the AraC/XylS family that share amino acid sequence similarity with AraC over its entire length (9, 13, 28). Based on this similarity, RhaS and RhaR are predicted to consist of two domains connected by a flexible linker (5, 12, 29, 41). The N-terminal domains are predicted to be responsible for L-rhamnose-binding and dimerization, while the C-terminal domains contain the 99 amino acid region that classifies them as members of the AraC/XylS family. In all studied cases of AraC/XylS family members, including RhaS and RhaR, the characteristic 99 amino acid region constitutes a DNA binding domain (3, 10, 43). This DNA-binding domain has also been shown to be involved in transcription activation in a number of AraC/XylS family proteins including Ada, RhaS, AraC, MelR, MarA, SoxS, XylS, and UreR (1, 4, 5, 15, 16, 20-22, 37).

In this paper, we further explored the mechanisms of transcription activation by RhaR and RhaS. We identified amino acids residues in the C-terminal domain of \square^{70} and in RhaR that are important for RhaR-mediated transcription activation at the *rhaSR* promoter. We then used a genetic loss-of-contact approach to identify an interaction between RhaR D276 and \square^{70} R599 that is required for RhaR-mediated activation. We also extended the previous studies by Bhende and Egan (4) of RhaS-mediated transcription activation at *rhaBAD*. Here we identified a second interaction between RhaS and \square^{70} , in this case, RhaS D250 and \square^{70} K593.

MATERIALS AND METHODS

Culture media and conditions. *E. coli* cultures for β -galactosidase assays were grown in MOPS buffered medium (4, 34). Tryptone-yeast extract (TY) liquid medium (0.8% tryptone; 0.05% yeast extract; and 0.05% NaCl) was used to grow cells for most other experiments. SacB selection media (1% tryptone; 0.5% yeast extract; 1.5% agar; and 5% sucrose; pH 7.8) was used to select against *sacB*⁺ strains (14). Antibiotics were used as indicated at the following concentrations: ampicillin (200 μ g/ml), chloramphenicol (25 μ g/ml), kanamycin (25 μ g/ml), and tetracycline (20 μ g/ml).

General Methods. Standard methods were used for restriction endonuclease digestion and ligation using restriction endonucleases and T4 DNA ligase purchased from New England Biolabs (Beverly, MA). Transformation was carried out using chemically induced competent cells of *E. coli* and plasmid DNA was purified by alkaline lysis. DNA sequencing reactions were carried out using custom-synthesized IRD41 dye-labeled primers (Table 2) from LI-COR Inc. (Lincoln, NE) and the Thermo Sequenase primer cycle sequencing kit from Amersham Life Sciences (Arlington Heights, IL). DNA sequences were analyzed by automated di-deoxy sequencing on a LI-COR 4000L sequencer (University of Kansas Biochemical Research Service Laboratory). The Expand High Fidelity PCR System (Roche; Indianapolis, IN) was used to amplify DNA fragments for cloning as well as to generate template for DNA sequencing from *rhaS* and *rhaR* alleles that were recombined into the chromosome. The DNA sequence of both strands was determined for the entire cloned region of all cloned, mutagenized, and recombined DNA fragments. The QIAquick PCR Purification Kit (Qiagen; Chatsworth, CA) was used to clean up PCR products.

Strains, plasmids and phage. Table 1 lists the strains, phage, and plasmids used in this study. All strains used in β -galactosidase assays were derived from ECL116 (2) and carried *lacZ* fusions in single copy on λ phage integrated at *att λ* (40). P1 phage-mediated generalized transduction was used to move λ (*recC ptr recB recD*)::*Plac-bet exo*

kan (from KM22) into SME1216 (selecting for kanamycin resistance) to make SME2417. SME2495 was made using P1 transduction to move $\square(rhaSR)::kan\ zih-35::Tn10$ (from SME2800) in SME1217 selecting for tetracycline resistance and then screening for a Rha⁻ phenotype. SME2496 was made from SME2416 by transformation with a PCR product containing $\square(rhaSR)::cat-sac$ (amplified from pSE254 – described below), which was recombined onto the chromosome using the recombination genes of bacteriophage \square (encoded by $\square(recC\ ptr\ recB\ recD)::Plac-bet\ exo\ kan$)(31). The plasmid pSE250 was made by restriction endonuclease digestion of pSE101 with BamHI at the *rhaT'* end of the clone and EcoRI (a natural site within the *rhaBAD* promoter) creating the fragment *rhaSRT'*, which was purified from an agarose gel using Qiagen's QIAEX Gel Extraction Kit. The *rhaSRT'* fragment was then ligated to pUC18 (46) which had been digested with BamHI and EcoRI. To make pSE254, long-way around PCR using pSE250 as template and primers 2297 and 2298 amplified all of the pSE250 sequence except *rhaSR* and added a BglIII site at each end. Then PCR with primers 2299 and 2300, using a PCR product containing the *cat-sac* cassette (provided by Kenan Murphy (32)) as template, generated a product that was ligated to the BglIII sites of the long-way around PCR product to create pSE254. Plasmids pML148-169 (containing mutations in the *rpoD* gene) were obtained from the laboratory of Carol Gross and were sequenced to ensure they still carried the expected mutations. Several of the *rpoD* alleles were initially found to be wild-type. Assays involving these alleles were repeated upon obtaining true mutants.

Mutagenesis of *rhaS* and *rhaR*. The mutant *rhaS* D250A allele was moved from pSE172 into the context of pSE101 by digesting pSE172 with BstEII and BglIII (both sites are native to the wild-type *rhaS* gene) to create a fragment encoding the RhaS D250A substitution. This fragment was then ligated to similarly digested pSE101 to make pSE249. Genes encoding alanine substitution derivatives of RhaR D276A and RhaR D285A were constructed by oligonucleotide-directed mutagenesis of *rhaR* in pGEM-

11Zf(+ (Promega; Madison, WI) using the GeneEditor kit (Promega) and oligonucleotides 2208 and 2210. The mutant *rhaR* alleles were then subcloned to pSE250 using NheI and SmaI restriction endonuclease sites (both sites occur naturally within *rhaR*) to make pSE251 and pSE253. The *rhaR* E284A mutagenesis was performed using PCR to make oligonucleotide-directed mutations at the desired position with primer 2381, which also contained the recognition sequence for the EarI restriction endonuclease. Second, a non-mutagenized PCR fragment was made, also using a primer with EarI restriction sites. Finally, ligation of the mutant and wild-type DNA fragments allowed seamless reconstruction (25) of the full-length *rhaR* E284A gene in the context of *rhaSRT'* to make pSE252. Oligos Etc (Wilsonville, OR), Integrated DNA Technologies (Coralville, IA), and MWG-Biotech (High Point, NC) synthesized oligonucleotide primers used in mutagenesis (Table 2). Mutations were initially identified by diagnostic PCR using the following method. The very 3' nucleotides of the diagnostic oligonucleotide contained the desired substitution(s) such that amplification was only possible (in combination with a suitable downstream primer) when the template DNA carried the desired mutation. Putative mutants identified by this method were confirmed by DNA sequencing of both strands of the entire cloned region (see Table 2 for sequencing oligonucleotides).

Recombination of *rhaS* and *rhaR* alleles onto the chromosome. The mutant *rhaS* and *rhaR* alleles constructed as described above were recombined onto the *E. coli* chromosome such that they replaced the wild type *rhaS* or *rhaR* alleles using the following methods. Each *rhaS* or *rhaR* mutant was present on a plasmid in the context of *rhaSRT'* (pSE249, pSE251, pSE252, and pSE253). Oligonucleotides 1170 and 2292 were used to amplify each mutant *rhaSRT'* region by high-fidelity PCR. Approximately 500 ng of the *rhaSRT'* PCR product carrying a mutant allele was used to transform either SME2495 [□ (□ *rhaB-lacZ*) □110, □(*recC ptr recB recD*)::Plac-*bet* *exo kan*, □(*rhaSR*)::*kan*, *zih-35*::Tn10] or SME2496 [□ □(*rhaB-lacZ*) □110, □(*recC ptr recB recD*)::Plac-

bet *exo kan*, $\square(rhaSR)::cat-sac, zih-35::Tn10]$. Since SME2495 and SME2496 both contained P_{lac} -*bet* *exo*, which encodes the \square phage recombination proteins, the frequency of homologous recombination was much higher in these strains than in wild-type *E. coli* strains (31). The transformants were screened by spread plating on media containing X-gal (40 \square g/ml) and L-rhamnose (0.2%) to identify functional, or partially functional, *rhaSR* genes that replaced the $\square(rhaSR)$ allele. There was no selection for successful recombinants in SME2495, rather we screened for blue colonies amongst a lawn of white colonies. When transforming SME2496, which contains a *cat-sacB* cassette (32) in place of *rhaSR*, we selected for the sucrose resistance of cells that had lost the *sacB* gene (which confers sucrose sensitivity) by homologous recombination. However, due to a significant background of spontaneous sucrose resistant mutants, the transformants were also screened for at least partially functional *rhaS* or *rhaR* genes by adding X-gal (40 \square g/ml) and L-rhamnose (0.2%) to the SacB selection plates. We found that sucrose inhibition of the *sacB*⁺ cells worked most reproducibly at room temperature, although it took about 3 days for the cells to grow. Phage P1-mediated generalized transduction was then used to transfer the *rhaS* or *rhaR* allele of interest (linked to *zih-35::Tn10*) to either 1851 [\square $\square(rhaB-lacZ)$ \square 84] or 2515 [\square $\square(rhaS-lacZ)$ \square 92] by selecting for the tetracycline resistance conferred by *zih-35::Tn10*. Diagnostic PCR, as described above, was used to initially identify transductants that contained the *rhaS* or *rhaR* mutation of interest. High fidelity PCR was then used to amplify *rhaSRT'* from the chromosome using oligonucleotides 2097 and 1170, and the entire 3kb PCR product was sequenced, as described above, to verify the presence of the desired mutation with no additional mutations. Phage P1-mediated transduction was then used to introduce *recA::kan* into each strain to make SME2689, 2691, 2692, and 2933. Finally, competent cells of each strain were made and transformed with plasmids containing either the wild type-, K593A-, L595A-, R599A-, or R608A-encoding \square^{70} genes for \square -galactosidase assays.

β-Galactosidase assay. β-galactosidase assays were performed as previously described (3). In all cases, chromosomal *rpoD* was expressed from its own promoter, not the *trp* promoter described in Lonetto et al. (27), and the plasmid encoded β⁷⁰ derivatives were expressed in the absence of IPTG. Under these conditions, the β⁷⁰ derivatives are expected to account for approximately 50% of the total β⁷⁰ in the cells (27). Specific activities were averaged from at least three independent assays with two replicates in each assay. The assays were performed on at least two different days, with independent cell growth steps (starter TY culture, overnight culture, and final growth culture) for each assay.

RESULTS

σ^{70} derivatives at the *rhaSR* promoter. We wished to determine whether any residues near the C-terminal end of σ^{70} were important for transcription activation by RhaR. Lonetto *et al.* (27) constructed a library of alanine substitutions at 17 different positions near the C-terminus of σ^{70} and found that some substitutions resulted in defects at class II activator-dependent promoters. Previous work from our lab found that two of the alanine substitutions in this library were defective at a truncated *rhaBAD* promoter where RhaS was the only transcription activator (4). We assayed this library of alanine substitutions in σ^{70} at two RhaR-activated single-copy translational fusions, $\square(rhaS-lacZ)\square_{216}$ and $\square(rhaS-lacZ)\square_{92}$. The $\square(rhaS-lacZ)\square_{216}$ promoter contained the RhaR binding site as well as upstream CRP sites, while the $\square(rhaS-lacZ)\square_{92}$ promoter contained only the RhaR binding site (Fig. 1). Since the assays were carried out in a strain that also expressed wild-type σ^{70} from the chromosome (27), we considered values below 80% of wild-type activity to be significant defects. At $\square(rhaS-lacZ)\square_{216}$, σ^{70} derivative L595A had 66% of the activity of wild-type σ^{70} (Fig. 2A), while the remaining σ^{70} derivatives were not significantly defective. When the same sigma derivatives were assayed at $\square(rhaS-lacZ)\square_{92}$, L595A was still significantly defective, with 53% activity compared to wild-type σ^{70} (Fig. 2B). In addition, three alanine substitutions of positively charged amino acid residues, K593A (79%), R599A (48%), and R608A (77%) were defective at $\square(rhaS-lacZ)\square_{92}$. These results suggested that σ^{70} residues K593, L595, R599, and R608 might make protein-protein contacts with RhaR that are required for transcription activation. The lack of defect by σ^{70} K593A, R599A, or R608A at the $\square(rhaS-lacZ)\square_{216}$ promoter is similar to previous findings with RhaS and AraC that substitutions at some σ^{70} residues were only defective in the absence of CRP activation (4, 27).

Based on the previous finding in our lab that a contact between RhaS residue D241 and \square^{70} residue R599 is required for full transcription activation by RhaS (4), we predicted that RhaR D276, which aligns with RhaS D241 (Fig. 3), might contact \square^{70} R599 at the *rhaSR* promoter. Molecular modeling of the RhaR- \square^{70} interaction (Fig. 4) indicates that the negatively charged RhaR residue D276 is very close to the positively charged \square^{70} residue R599. RhaR D276 is also near \square^{70} R608, although in the model they do not appear close enough to interact. The molecular model further shows that two adjacent negatively charged RhaR residues, E284 and D285, were located near \square^{70} K593. Based on these pieces of evidence, we hypothesized that contacts between some or all of the RhaR residues D276, E284, and D285 and \square^{70} might be required for maximal transcription activation by RhaR. We therefore tested alanine substitutions at these positions in RhaR for defects in transcription activation.

RhaR residues D276, E284, and D285 are important for *rhaSR* transcription activation. In order to test whether the side chains of RhaR residues D276, E284, and D285 might play a role in transcription activation by RhaR, we constructed alanine substitutions at each of these positions. If the amino acid residues at these positions are required for transcription activation, the alanine substitution should result in a significant decrease in activation of *rhaSR* transcription. To assay the RhaR derivatives, the mutant *rhaR* alleles on plasmids were first recombined onto the chromosome such that they replaced the wild-type *rhaR* gene (see Materials and Methods). The wild-type and mutant *rhaR* alleles were then assayed for activation of \square (*rhaS-lacZ*) \square_{92} (Fig. 5). The results showed that all three of the alanine substitutions in RhaR were significantly defective, highlighting the importance of the wild-type residues at those positions. The especially large defect of RhaR D285A may be partly due to a role in DNA-binding based on its alignment with D250 in RhaS (Fig. 3), which makes base-specific contacts with DNA (3). However, a role in DNA-binding for RhaR D285 does not rule out

interactions with \square^{70} , therefore all three of these RhaR residues are candidates for specific contacts with \square^{70} .

Evidence for an interaction between RhaR D276 and \square^{70} R599. We used a genetic loss-of-contact approach to test potential interactions between RhaR D276 and \square^{70} K593 or R599. Using this approach, we separately combined wild-type RhaR or the RhaR D276A derivative with each of three plasmids encoding either \square^{70} wild-type, K593A, or R599A in a strain carrying single copy $\square(rhaS-lacZ)\square_{92}$. The results shown in Fig. 6A were graphed so that the activity with wild-type \square^{70} was set to 100% for each RhaR derivative, thereby illustrating the relative effects of each \square^{70} derivative. On this graph, therefore, a \square^{70} derivative that does not define a site of interaction with a given RhaR derivative is expected to have the same relative defect when combined with the indicated RhaR derivative as it does with wild-type RhaR, since the defects will be independent of each other. On the other hand, if a \square^{70} derivative does define a site of interaction with a given RhaR derivative, the \square^{70} derivative will confer no further defect when combined with the indicated RhaR derivative, since the interaction would already have been lost with the RhaR derivative. Using this method to analyze the results in Fig. 6A, our first conclusion is that there is no interaction between RhaR D276 and \square^{70} K593 since the \square^{70} K593A derivative had approximately the same relative defect in combination with either wild-type RhaR or RhaR D276A. Therefore, the defects of \square^{70} K593A and RhaR D276A are independent. These results and those in Fig. 2B also show that the \square^{70} R599A derivative by itself (in a wild-type *rhaR* strain) had approximately 50% activity compared to wild-type \square^{70} . However, when \square^{70} R599A was combined with RhaR D276A, the \square^{70} R599A derivative conferred no further defect upon RhaR D276A. In fact, the strain with the combination of \square^{70} R599A and RhaR D276A had approximately 1.7-fold higher activity than the strain with wild-type \square^{70} and RhaR D276A. These results fit the criteria for an allele-specific contact between \square^{70} R599 and RhaR D276. As mentioned above, molecular modeling is consistent with this

interaction since RhaR D276 is in close proximity to \square^{70} R599 in the model (Fig. 4). We also tested the \square^{70} R608A derivative in combination with RhaR D276A and found that it had the same relative defective as it did with wild-type RhaR (79% of wild-type \square^{70} activity in both cases – not shown), therefore there was no indication of an interaction between these two residues.

RhaR E284 and D285 and \square^{70} . Using the same genetic loss-of-contact approach, we also tested for potential interactions between \square^{70} and RhaR E284 and D285. The results in Fig. 6B show that the K593A \square^{70} derivative was not defective in combination with RhaR D285A (104% of wild-type \square^{70} activity), but the R599A \square^{70} derivative also became less defective (81% of wild-type \square^{70} activity). In the absence of the results with \square^{70} 599A, one might conclude that RhaR D285 contacts \square^{70} K593, since \square^{70} K593A had no significant defect when combined RhaR D285A, however, the lack of strict allele specificity sheds doubt on this conclusion. To further investigate the non-allele specific defects of \square^{70} substitutions in combination with RhaR D285A, we tested \square^{70} L595A and R608A derivatives, which were both defective in a wild-type *rhaR* strain, as shown in Fig. 2B. When combined with RhaR D285A, the \square^{70} L595A and R608A derivatives were not significantly defective with 86% and 87% of wild-type \square^{70} activity, respectively (not shown). These results suggest that RhaR D285A may reduce the ability of RhaR to interact with \square^{70} in a non-allele specific manner; therefore, we can't conclude whether RhaR D285 contacts any of these \square^{70} residues.

Fig. 6C shows the results of assays to identify potential interactions involving RhaR E284. Our results showed that neither \square^{70} K593A nor R599A conferred a significant defect on RhaR E284A. In fact, the \square^{70} K593A-RhaR 284A combination gave much higher activity (362%) than the RhaR 284A derivative with wild-type \square^{70} . Therefore, as above, we tested the \square^{70} L595A and R608A derivatives in the *rhaR* E285A strain and measured 139% and 93% activity, respectively, compared to wild-type \square^{70} (not shown). Thus, we again found that all four of the \square^{70} derivatives that were

defective in the wild-type *rhaR* strain were no longer significantly defective in the *rhaR* E284A strain. These results suggest that, similar to RhaR D285A, the RhaR E284A derivative may reduce the ability of RhaR to interact with \square^{70} in a non-allele specific manner. One explanation for the very high relative activity of RhaR E284A in combination with \square^{70} K593A is that a new interaction may have been created in this case.

Evidence for a specific interaction between RhaS D250 and \square^{70} . Our lab previously identified an interaction between RhaS D241 and \square^{70} R599, and we also found that \square^{70} K593A was defective at \square (*rhaB-lacZ*) \square ⁸⁴ but did not identify an amino acid in RhaS that might contact \square^{70} K593 (4). The molecular model in Fig. 4 shows that the only negatively charged RhaS residue that is in close proximity to the positively charged \square^{70} K593 is RhaS D250, suggesting that these two residues might make a contact. Previous results from our lab showed that RhaS D250A was 12-fold defective for \square (*rhaB-lacZ*) \square ⁸⁴ activation, however, they also indicated that this residue participates in a base-specific DNA contact (3). In contrast to other approaches to identify positive control mutants, the genetic loss-of-contact approach does not require that the protein have wild-type DNA-binding capability, hence it has the potential to identify residues that have dual DNA-binding and transcription activation functions. We therefore used the genetic loss-of-contact approach to test whether RhaS D250 and \square^{70} K593 might be involved in an interaction. The results (Fig. 6D) support the hypothesis of an interaction between RhaS D250 and \square^{70} K593 since the K593A derivative was not significantly defective when combined with RhaS D250A (87% activity compared to wild-type \square^{70}). However, when \square^{70} R599A was combined with RhaS D250A, it maintained approximately the same relative defect as it had with wild-type RhaS. These results suggest that there is an allele-specific interaction between RhaS D250 and \square^{70} K593. Molecular modeling is consistent with this interaction since, as mentioned above, RhaS D250 is in close proximity to \square^{70} K593 in the model (Fig. 4).

DISCUSSION

The C-terminus of σ^{70} is important for RhaS- and RhaR-mediated transcription activation. The binding sites for both RhaS and RhaR overlap the –35 region of their respective core promoters by four base pairs placing them in ideal positions to interact with the σ^{70} subunit of RNAP. Previous results by Bhende and Egan (4) identified two amino acid residues in σ^{70} , K593 and R599, that were important for RhaS-mediated transcription activation at *rhaBAD* and *rhaT*. In this study, we identified four amino acid residues in σ^{70} , K593, L595, R599, and R608 which were important for RhaR-mediated transcription activation of *rhaSR* (Fig. 2B). Two of the alanine substitutions in σ^{70} , K593A and R599A, were defective at all three of the *rha* promoters suggesting similar mechanisms of activation by RhaS and RhaR.

The results in this paper (Fig. 2) as well as those from the previous study (4) showed that σ^{70} K593A and R599A were only defective at truncated *rha* promoters that did not include the upstream CRP binding sites. This is similar to the findings at several other promoters that require multiple activators, such as *araBAD*, *uhpT* and *narG* (18, 27, 36, 39). Two possible explanations for this trend are that the second activator increases the total number of interactions such that the relative importance of each individual interaction decreases, or that the second activator creates redundancies in activation that mask the importance of other interactions. A third possibility is that the second activator alters the orientation of the first activator relative to σ^{70} such that the primary activator is no longer in an ideal position to interaction with σ^{70} . In the first two models, the activator interaction with σ^{70} occurs both in the presence and absence of the second activator, but can only be detected in its absence, whereas in the third model, the interaction between the first activator and σ^{70} only occurs in the absence of the second activator. Further experiments will be needed to distinguish these models. At the *rhaSR* promoter, the σ^{70} L595A derivative was unique in that it was defective both in

the presence and absence of the second activator, CRP, but it's role in RhaR-mediated transcription activation is not yet known.

Specific amino acid contacts between \square^{70} and RhaR. Previous results showing an interaction between RhaS D241 and \square^{70} R599 at *rhaBAD* (4) led us to investigate whether an interaction between RhaR D276 and \square^{70} R599 might be required for RhaR activation at *rhaSR*. We also used a molecular model of the RhaR- \square^{70} domain 4 interaction in which the structure of MarA (38) represented RhaR (Fig. 4), to identify the only two negatively charged RhaR residues, E284 and D285, that were near \square^{70} K593. RhaR E284 and D285 were therefore considered candidates for residues that might interact with \square^{70} K593. After determining that alanine substitutions at RhaR residues D276, E284, and D285 were all defective for *rhaSR* activation (Fig. 5), we used a genetic loss-of-contact approach to test for specific amino acid interactions between \square^{70} and RhaR.

To carry out a loss-of-contact analysis, one must first identify defective derivatives of each of the potentially interacting proteins. In the simplest case, the full defect of both of the two interacting residues is due to loss of the interaction – in other words, the only role of the two residues is the interaction. The rationale behind this approach in this simple case is that mutation of one or the other of the interacting residues will eliminate the interaction, therefore, the phenotype of a strain carrying both mutations will be the same as the phenotype of the strains carrying the individual mutations. If one of the residues has a second role in addition to the interaction, then the strain carrying both mutations will have a phenotype that is no worse than the more defective of the strains carrying the two individual mutations. This analysis does not provide conclusive results if both residues have roles in addition to the interaction. It is also expected that the predicted interactions will be allele specific. The majority of combinations of defective derivatives are not expected to identify interacting residues;

and in these cases the defects resulting from each of the two mutations will at least be additive.

Using this rationale to interpret our genetic loss-of-contact assays, the results in Fig. 6A provide evidence for an interaction between \square^{70} R599 and RhaR D276. This result is similar to previous results from our lab (4) that indicate an interaction between \square^{70} R599 and RhaS D241 and evidence from Grainger et al. that \square^{70} R599 interacts with MelR D261 (16), which aligns with RhaS D241 and RhaR D276. Molecular modeling of the RhaR- \square^{70} complex (Fig. 4) shows that \square^{70} R599 and RhaR D276 are in close proximity, consistent with our interpretation that these two residues interact. Our genetic loss-of-contact results do not provide evidence for an interaction between \square^{70} K593 and RhaR E284 or D285 (Fig. 6C). Instead, our results indicate that alanine substitutions at RhaR E284 and D285 result in non-allele specific decreases in the defects of all of the \square^{70} alleles tested. One hypothesis is that RhaR E284A and D285A alter the details of the RhaR DNA interaction such that RhaR is no longer in an ideal position to interact with \square^{70} domain 4.

The role of \square^{70} K593 in transcription activation by RhaS. Residue K593 of \square^{70} has been found to be important for several transcription activators, including AraC, UhpA, \square cI, FNR, Ada, RhaR (this study), and RhaS (4, 24, 27, 35, 36). With the exception of \square cI and RhaS (this study), evidence that \square^{70} K593 directly contacts an activator has not been obtained. Our results indicate that \square^{70} K593 contacts RhaS D250 as a part of the mechanism of activation by RhaS (Fig. 6D). Our molecular model of the RhaS- \square^{70} interaction shows that \square^{70} K593 and RhaS D250 are in close proximity, consistent with this result (Fig. 4). While the binary complex of Taq \square^A domain 4 and DNA shows that the residue that corresponds to \square^{70} K593 contacts DNA, in the \square cI/ \square domain 4/DNA ternary complex this residue participates in a protein-protein contact with \square cI instead (6, 19). These findings indicate that \square^{70} K593 is capable of interacting with an

appropriately positioned transcription activator, and are consistent with our proposal that \square^{70} K593 may contact RhaS D250.

Comparison of transcription activation by RhaS and RhaR. In this study we have identified an interaction between RhaR D276 and \square^{70} R599 that is equivalent to our previously identified interaction of RhaS D241 and \square^{70} R599. Further, although a RhaR equivalent of the RhaS D250 interaction with \square^{70} K593 was not identified, our results do not rule out that such an interaction occurs with RhaR. Therefore, our current evidence suggests that the RhaS- \square^{70} interface is similar to the RhaR- \square^{70} interface. We certainly expect, however, that not all aspects of RhaS activation and RhaR activation will be identical. For example, we know that the CRP site at *rhaBAD* is centered at position -92.5, whereas the most important CRP site at *rhaSR* is centered at position -111.5. It is not possible to draw conclusions about how or whether differences in the RhaS- \square^{70} and RhaR- \square^{70} interfaces might relate to this difference in CRP binding site position, since all but one of the \square^{70} derivatives tested were only defective in the absence of CRP. However, it is likely that there is a difference in the mechanisms of RhaS and RhaR activation that relates to this difference in the positions of the CRP binding sites.

ACKNOWLEDGMENTS

We would like to thank Carol Gross for the library of alanine substitutions in \square^{70} , Richard Wolf for alerting us that some of the \square^{70} mutants had reverted to wild-type, Kenan Murphy for providing strain KM22 and the *cat-sacB* cassette, Jeff Urbauer for assistance with the modeling of \square^{70} domain 4 into the MarA-DNA structure, and Vydehi Rao for performing the assays of the \square^{70} library in the strain containing $\square(rhaS-lacZ)\square^{92}$.

This work was supported by Public Health Service grant GM55099 from the National Institute of General Medical Sciences and NIH Grant RR-P20 RR17708 from the Institutional Development Award (IDeA) Program of the National Center for Research Resources, both to S.M.E.

REFERENCES

1. **Akimaru, H., K. Sakumi, T. Yoshikai, M. Anai, and M. Sekiguchi.** 1990. Positive and negative regulation of transcription by a cleavage product of Ada protein. *J Mol Biol* **216**:261-73.
2. **Backman, K., Y.-M. Chen, and B. Magasanik.** 1981. Physical and genetic characterization of the *gln A-glnG* region of the *Escherichia coli* chromosome. *Proc. Nat. Acad. Sci., U.S.A.* **78**:3743-3747.
3. **Bhende, P. M., and S. M. Egan.** 1999. Amino acid-DNA contacts by RhaS: an AraC family transcription activator. *J. Bacteriol.* **181**:5185-5192.
4. **Bhende, P. M., and S. M. Egan.** 2000. Genetic evidence that transcription activation by RhaS involves specific amino acid contacts with sigma 70. *J. Bacteriol.* **182**:4959-4969.
5. **Bustos, S. A., and R. F. Schleif.** 1993. Functional domains of the AraC protein. *Proc. Natl. Acad. Sci. USA* **90**:5638-5642.
6. **Campbell, E. A., O. Muzzin, M. Chlenov, J. L. Sun, C. A. Olson, O. Weinman, M. L. Trester-Zedlitz, and S. A. Darst.** 2002. Structure of the bacterial RNA polymerase promoter specificity σ subunit. *Mol. Cell* **9**:527-39.
7. **Dhiman, A., and R. Schleif.** 2000. Recognition of overlapping nucleotides by AraC and the sigma subunit of RNA polymerase. *J. Bacteriol.* **182**:5076-81.
8. **Dove, S. L., S. A. Darst, and A. Hochschild.** 2003. Region 4 of sigma as a target for transcription regulation. *Mol Microbiol* **48**:863-74.
9. **Egan, S. M.** 2002. Growing repertoire of AraC/XylS activators. *J Bacteriol* **184**:5529-32.
10. **Egan, S. M., and R. F. Schleif.** 1994. DNA-dependent renaturation of an insoluble DNA binding protein. Identification of the RhaS binding site at *rhaBAD*. *J. Mol. Biol.* **243**:821-829.

11. **Egan, S. M., and R. F. Schleif.** 1993. A regulatory cascade in the induction of *rhaBAD*. *J. Mol. Biol.* **234**:87-98.
12. **Eustance, R. J., S. A. Bustos, and R. E. Schleif.** 1994. Reaching out: Locating and lengthening the interdomain linker in AraC protein. *J. Mol. Biol.* **242**:330-338.
13. **Gallegos, M.-T., R. Schleif, A. Bairoch, K. Hofmann, and J. L. Ramos.** 1997. AraC/XylS family of transcriptional regulators. *Microbiol. Mol. Biol. Rev.* **61**:393-410.
14. **Gay, P., D. Le Coq, M. Steinmetz, T. Berkelman, and C. I. Kado.** 1985. Positive selection procedure for entrapment of insertion sequence elements in gram-negative bacteria. *J. Bacteriol* **164**:918-21.
15. **Grainger, D. C., T. A. Belyaeva, D. J. Lee, E. I. Hyde, and S. J. Busby.** 2004. Transcription activation at the *Escherichia coli* melAB promoter: interactions of MelR with the C-terminal domain of the RNA polymerase alpha subunit. *Mol Microbiol* **51**:1311-20.
16. **Grainger, D. C., C. L. Webster, T. A. Belyaeva, E. I. Hyde, and S. J. Busby.** 2004. Transcription activation at the *Escherichia coli* melAB promoter: interactions of MelR with its DNA target site and with domain 4 of the RNA polymerase sigma subunit. *Mol Microbiol* **51**:1297-309.
17. **Holcroft, C. C., and S. M. Egan.** 2000. Interdependence of activation at *rhaSR* by cyclic AMP receptor protein, the RNA polymerase alpha subunit C-terminal domain and RhaR. *J. Bacteriol.* **182**:6774-6782.
18. **Hu, J. C., and C. A. Gross.** 1985. Mutations in the sigma subunit of *E. coli* RNA polymerase which affect positive control of transcription. *Mol. Gen. Genet.* **199**:7-13.
19. **Jain, D., B. E. Nickels, L. Sun, A. Hochschild, and S. A. Darst.** 2004. Structure of a Ternary Transcription Activation Complex. *Molecular Cell* **13**:45-53.

20. **Jair, K., R. G. Martin, J. L. Rosner, N. Fujita, A. Ishihama, and R. E. Wolf, Jr.** 1995. Purification and regulatory properties of MarA protein, a transcriptional activator of *Escherichia coli* multiple antibiotic and superoxide resistance promoters. *J. Bacteriol.* **177**:7100-7104.
21. **Jair, K.-W., W. P. Fawcett, N. Fujita, A. Ishihama, and R. E. Wolf, Jr.** 1996. Ambidextrous transcriptional activation by SoxS: requirement for the C-terminal domain of the RNA polymerase alpha subunit in a subset of *Escherichia coli* superoxide-inducible genes. *Molec. Microbiol.* **19**:307-317.
22. **Kaldalu, N., U. Toots, V. de Lorenzo, and M. Ustav.** 2000. Functional domains of the TOL plasmid transcription factor XylS. *J. Bacteriol.* **182**:1118-26.
23. **Kuldell, N., and A. Hochschild.** 1994. Amino acid substitutions in the -35 recognition motif of σ^{70} that result in defects in phage λ repressor-stimulated transcription. *J. Bacteriol.* **176**:2991-2998.
24. **Landini, P., and S. J. Busby.** 1999. The *Escherichia coli* Ada protein can interact with two distinct determinants in the σ^{70} subunit of RNA polymerase according to promoter architecture: Identification of the target of Ada activation at the *alkA* promoter. *J. Bacteriol.* **181**:1524-1529.
25. **LaPointe, C. F., and R. K. Taylor.** 2000. The type 4 prepilin peptidases comprise a novel family of aspartic acid proteases. *J Biol Chem* **275**:1502-10.
26. **Li, M., H. Moyle, and M. M. Susskind.** 1994. Target of the Transcriptional Activation Function of Phage λ cI Protein. *Science* **263**:75-77.
27. **Lonetto, M. A., V. Rhodius, K. Lamberg, P. Kiley, S. Busby, and C. Gross.** 1998. Identification of a contact site for different transcription activators in region 4 of the *Escherichia coli* RNA polymerase σ^{70} subunit. *J. Mol. Biol.* **284**:1353-1365.
28. **Martin, R. G., and J. L. Rosner.** 2001. The AraC transcriptional activators. *Curr. Opin. Microbiol.* **4**:132-7.

29. **Menon, K. P., and N. L. Lee.** 1990. Activation of ara operons by a truncated AraC protein does not require inducer. *Proc Natl Acad Sci U S A* **87**:3708-12.
30. **Meyer, B. J., R. Maurer, and M. Ptashne.** 1980. Gene regulation at the right operator (OR) of bacteriophage lambda. II. OR1, OR2, and OR3: their roles in mediating the effects of repressor and cro. *J Mol Biol* **139**:163-94.
31. **Murphy, K. C.** 1998. Use of bacteriophage λ recombination functions to promote gene replacement in *Escherichia coli*. *J. Bacteriol.* **180**:2063-2071.
32. **Murphy, K. C., K. G. Campellone, and A. R. Poteete.** 2000. PCR-mediated gene replacement in *Escherichia coli*. *Gene* **246**:321-30.
33. **Nakabeppu, Y., and M. Sekiguchi.** 1986. Regulatory mechanisms for induction of synthesis of repair enzymes in response to alkylating agents: ada protein acts as a transcriptional regulator. *Proc Natl Acad Sci U S A* **83**:6297-301.
34. **Neidhardt, F. C., P. L. Bloch, and D. F. Smith.** 1974. Culture medium for enterobacteria. *J. Bacteriol.* **119**:736-747.
35. **Nickels, B. E., S. L. Dove, K. S. Murakami, S. A. Darst, and A. Hochschild.** 2002. Protein-protein and protein-DNA interactions of sigma70 region 4 involved in transcription activation by lambdacl. *J Mol Biol* **324**:17-34.
36. **Olekhovich, I. N., and R. J. Kadner.** 1999. RNA Polymerase σ and σ^{70} subunits Participate in Transcription of the *Escherichia coli* *uhpT* Promoter. *J Bact* **181**:7266-7273.
37. **Poore, C. A., C. Coker, J. D. Dattelbaum, and H. L. Mobley.** 2001. Identification of the domains of UreR, an AraC-like transcriptional regulator of the urease gene cluster in *Proteus mirabilis*. *J Bacteriol* **183**:4526-35.
38. **Rhee, S., R. G. Martin, J. L. Rosner, and D. R. Davies.** 1998. A novel DNA-binding motif in MarA: the first structure for an AraC family transcriptional activator. *Proc. Natl. Acad. Sci. USA* **95**:10413-10418.

39. **Silverstone, A. E., M. Goman, and J. G. Scaife.** 1972. *ALT: A New Factor Involved in the Synthesis of RNA by Escherichia coli.* *Molec. Gen. Genet.* **118**:223-234.
40. **Simons, R. W., F. Houman, and N. Kleckner.** 1987. Improved single and multicopy *lac*-based cloning vectors for protein and operon fusions. *Gene* **53**:85-96.
41. **Soisson, S. M., B. MacDougall-Shackleton, R. Schleif, and C. Wolberger.** 1997. Structural basis for ligand-regulated oligomerization of AraC. *Science* **276**:421-425.
42. **Tobin, J. F., and R. F. Schleif.** 1987. Positive regulation of the *Escherichia coli* L-rhamnose operon is mediated by the products of tandemly repeated regulatory genes. *J. Mol. Biol.* **196**:789-799.
43. **Tobin, J. F., and R. F. Schleif.** 1990. Purification and properties of RhaR, the positive regulator of the L-rhamnose operons of *Escherichia coli*. *J. Mol. Biol.* **211**:75-89.
44. **Travers, A.** 1974. RNA polymerase--promoter interactions: some general principles. *Cell* **3**:97-104.
45. **Via, P., J. Badia, L. Baldoma, N. Obradors, and J. Aguilar.** 1996. Transcriptional regulation of the *Escherichia coli rhaT* gene. *Microbiology* **142**:1833-1840.
46. **Yanisch-Perron, C., J. Vieira, and J. Messing.** 1985. Improved M13 phage cloning vectors and host strains: nucleotide sequences of the M13mp18 and pUC19 vectors. *Gene* **33**:103-119.

TABLE 1. Strains used in this study.

Strain, phage or plasmid	Genotype	Source or reference
<i>E. coli</i> strains		
KM22	□(<i>recC ptr recB recD</i> ::P _{lac} - <i>bet exo kan</i>)	(31)
ECL116	F ⁻ □ <i>lacU169 endA hsdR thi</i>	(2)
SME1074	ECL116 □ SME106	Laboratory collection
SME1216	ECL116 □ SME103	Laboratory collection
SME1851	ECL116 □ SME104	Laboratory collection
SME2416	SME2417 <i>zih-35</i> ::Tn10	Laboratory collection
SME2417	SME1216 □(<i>recC ptr recB recD</i> ::Plac- <i>bet exo kan</i>)	This study
SME2495	SME2417 □ <i>rhaSR</i> :: <i>kan zih-35</i> ::Tn10	This study
SME2496	SME2416 □ <i>rhaSR</i> :: <i>cat-sacB</i>	This study
SME2508	ECL116 □ SME114 <i>recA</i> :: <i>cat</i>	Laboratory collection
SME2515	ECL116 □ SME114	Laboratory collection
SME2608	SME1851 <i>rhaS</i> (wild-type) <i>recA</i> :: <i>kan</i>	Laboratory collection
SME2689	SME1851 <i>rhaS</i> (D250A) <i>zih-35</i> ::Tn10 <i>recA</i> :: <i>kan</i>	This study
SME2691	SME2515 <i>rhaR</i> (D276A) <i>zih-35</i> ::Tn10 <i>recA</i> :: <i>kan</i>	This study
SME2692	SME2515 <i>rhaR</i> (D285A) <i>zih-35</i> ::Tn10 <i>recA</i> :: <i>kan</i>	This study
SME2693	SME2515 <i>rhaR</i> (wild-type) <i>recA</i> :: <i>kan</i>	This study
SME2800	SME1074 □ <i>rhaSR</i> :: <i>kan zih-35</i> ::Tn10	This study
SME2933	SME2515 <i>rhaR</i> (E284A) <i>zih-35</i> ::Tn10 <i>recA</i> :: <i>kan</i>	This study
Phage		
□RS45	<i>bla'</i> - <i>lacZ</i> _{sc} <i>att</i> ⁺ <i>imm</i> ²¹ <i>ind</i> ⁺	(40)
□ SME103	□ RS45 □ (<i>rhaB-lacZ</i>)□110	(11)
□ SME104	□ RS45□ (<i>rhaB-lacZ</i>)□84	(11)
□ SME106	□ RS45□ (<i>rhaS-lacZ</i>)□216	(11)
□ SME114	□ RS45 □ (<i>rhaS-lacZ</i>)□92	(17)
Plasmids		
pGEX-2T □ ⁷⁰	Ap ^r <i>rpoD</i> wild-type	(27)
pML148-169	pGEX-2T <i>rpoD</i> substitutions	(27)
pSE101	pTZ 18R Ap ^r <i>rhaSR+rhaBA'</i>	Laboratory collection
pSE172	Tet ^r pALTER-1 <i>rhaS</i> D250A	Laboratory collection
pSE249	pSE101 <i>rhaS</i> D250A	This study
pSE250	pUC18 <i>rhaSRT'</i> wild-type	This study
pSE251	pUC18 <i>rhaSRT'</i> <i>rhaR</i> D276A	This study
pSE252	pUC18 <i>rhaSRT'</i> <i>rhaR</i> E284A	This study
pSE253	pUC18 <i>rhaSRT'</i> <i>rhaR</i> D285A	This study
pSE254	pUC18 □ <i>rhaSR</i> :: <i>cat-sac</i>	This study
pUC18	Ap ^r <i>lacZ</i> □	(46)

TABLE 2. Oligonucleotides used in this study.

Oligo. No.	Oligonucleotide sequence, 5'-3'	Use
1170	<u>CCGGAATTC</u> TTGTGGTGATGTGATGCTCAC	Amplify <i>rhaSRT'</i> (within <i>rhaBAD</i> promoter)
2068	ATGACCGTATTACATAGTGTGGAT	IRD41 labeled - <i>rhaS</i> sequencing
2069	TTATTGCAGAAAGCCATCCCGTCC	IRD41 labeled - <i>rhaS</i> sequencing
2074	TGGTTGCACAGATGGAACAGC	IRD41 labeled - <i>rhaS</i> sequencing
2075	GTTGAGACGTGATGCGCTGTT	IRD41 labeled - <i>rhaS</i> sequencing
2097	<u>CGCGAATTC</u> AAGGGTATGGTTTTGCAG	Amplify <i>rhaSRT</i> from chromosome (within <i>rhaT</i> promoter)
2204	GGTCACCGCGTGATATTCG	IRD41 labeled - <i>rhaR</i> sequencing
2205	ATTCCGGGATTTAACGCCAG	IRD41 labeled - <i>rhaR</i> sequencing
2206	TTAATCTTTCTGCGAATTGAG	IRD41 labeled - <i>rhaR</i> sequencing
2207	CAAACGGCACATGCTGACTA	IRD41 labeled - <i>rhaR</i> sequencing
2208	CGGTCGAAAT <u>IG</u> CACTGATT	<i>rhaR</i> D276A mutagenesis
2210	AATAGTTACT <u>IG</u> CTTCAAAGCCAC	<i>rhaR</i> D285A mutagenesis
2292	<u>CCTGGATCCCCG</u> CAAAGTGAA	Amplify <i>rhaSRT'</i> from plasmids (within <i>rhaT</i>)
2297	<u>GGTAAGATCT</u> CGGTCATACTGGCCTCCTGATG	Long-way around PCR to delete <i>rhaSR</i>
2298	<u>GGTAAGATCT</u> TTAATTCGCCATGCCGATGCCGA	Long-way around PCR to delete <i>rhaSR</i>
2299	<u>GGTAAGATCT</u> CGGACCGGGTCGAATTTGC	Amplify <i>cat-sac</i> cassette
2300	<u>GGTAAGATCT</u> ATATCGGCATTTTCTTTTGCG	Amplify <i>cat-sac</i> cassette
2381	<u>ATTCTTCGTTGCGG</u> ATAGTAACTATTTTCGG TGGTG	<i>rhaR</i> E284A mutagenesis

^aRegions of oligonucleotides not complementary to wild-type DNA sequence (encode restriction endonuclease sites and flanking DNA or mutations) are underlined.

FIGURE LEGENDS

Fig. 1. Top: Representation of the divergent *rhaSR* and *rhaBAD* promoter regions showing the approximate positions of the transcription activators RhaS, RhaR and CRP as well as RNA polymerase at each promoter. Bottom: Three consecutive lines of DNA sequence extending from the *rhaSR* transcription start point to the *rhaBAD* transcription start point. Binding sites for RhaS, RhaR and CRP are shown by arrows and the -35 and -10 hexamers of each promoter are indicated. The upstream endpoints of promoter fusions used in this study are marked "□". Deletion end points, protein binding sites, and numbering relative to the *rhaSR* promoter are shown below the DNA sequence while deletion end points, protein binding sites, and numbering relative to the *rhaBAD* promoter are shown above the DNA sequence.

Fig. 2. Alanine substitutions within the C-terminal domain of the σ^{70} subunit of RNA polymerase assayed at two *rhaS-lacZ* fusions, □(*rhaS-lacZ*)□216 in SME1074 (A) and □(*rhaS-lacZ*)□92 in SME 2508 (B). The σ^{70} alanine substitutions were encoded on plasmids and the *rhaS-lacZ* fusions were in the chromosome as single-copy □ lysogens. In each panel, the values obtained with wild-type σ^{70} were set to 100% and the activity of each σ^{70} derivative is represented as a percentage of the wild-type σ^{70} value. In panel (A), the activity of wild-type σ^{70} was 86 Miller Units for the I590A, R596A, L598A, R603A, and R608A derivatives, while the wild-type σ^{70} activity for the other derivatives was 87 Miller Units. In panel (B), the wild-type σ^{70} activity was 3.6 Miller Units for the I590A, R596A, L598A, R603A, and R608A derivatives and 2.2 Miller Units for the other derivatives.

Fig. 3. Alignment of the amino acid sequences of the second helix-turn-helix DNA-binding motifs of RhaS and RhaR. Amino acids shown in black are those tested in this work for possible interactions with the σ^{70} subunit of RNAP. Identical amino acids are

indicated by vertical lines between the two sequences. The boundaries of the first helix (Helix 1), the turn, and the recognition helix (Helix 2) are based on the structure of MarA (38) and alignments between MarA and RhaS and RhaR. The numbers of the first and last residues shown, as well as those of the residues tested for interactions with \square^{70} are indicated.

Fig. 4. Model of RhaS or RhaR interactions with \square^{70} domain 4. The model of the RhaS or RhaR C-terminal domain (aqua) is based on the crystal structure of the MarA-DNA complex (38), while the model of \square^{70} domain 4 (yellow) is based on the crystal structure of the same domain of \square^A from *Thermus aquaticus* on DNA (6). Only the DNA from the MarA structure is shown (white). Amino acid residues in RhaS or RhaR and \square^{70} that are implicated in interactions are shown in space filling model and labeled, with the RhaS or RhaR residues colored red and the \square^{70} residues colored dark blue. The unlabeled space filling residues are RhaR E284 (pink), RhaR D285 (which is at the same position as RhaS D250), and \square^{70} R608 (light blue). Since \square^{70} sits in front of RhaS or RhaR when the DNA is shown parallel to the page, the model has been rotated somewhat around the vertical axis to allow a view between the interacting proteins. The modeling was performed using the program Insight II by first manually superimposing the DNA's in the pdf files of MarA on DNA (1BL0) and \square^A domain 4 on DNA (1KU7) such that the basepairs that corresponded to the -35 region of each were aligned as closely as possible. The \square^A model was then rotated to minimize clashes with MarA while maintaining the DNA superimposition. Finally, the residues implicated in interactions were highlighted. A second \square^A domain 4 molecule in the 1KU7 structure which does not make specific contacts with the DNA is not shown.

Fig. 5. Transcription activation by RhaR derivatives. \square -Galactosidase activity was assayed from a single copy fusion of the *rhaSR* promoter with *lacZ* that included the

RhaR binding site but not the CRP binding sites ($\square(rhaS-lacZ)\square92$). In each case, wild-type RhaR or the alanine substitutions in RhaR were encoded in the chromosome at the natural *rhaR* locus (strains SME2691, 2692, 2693, and 2933). The value obtained with wild-type RhaR (3.3 Miller units) was set to 100% and the activity of each RhaR derivative was represented as a percentage of that value.

Fig. 6. Combinations of RhaR or RhaS derivatives with \square^{70} derivatives. Plasmid-encoded \square^{70} alanine substitutions were combined with chromosomally-encoded alanine substitutions in RhaR or RhaS (strains SME 2689, 2691, 2692, 2693, and 2933) and \square -galactosidase activity was measured from $\square(rhaS-lacZ)\square92$ (A, B, C), or $\square(rhaB-lacZ)\square84$ (D). The activity of wild-type \square^{70} in combination with each RhaR or RhaS derivative in Miller Units is shown on the corresponding bar in each graph, and was set to 100% in each case. This representation allows the relative defects of the \square^{70} derivatives to be directly compared. The value for \square^{70} K593A in combination with RhaR E284A was 362% of the wild-type \square^{70} value and is drawn off-scale to prevent compression of the remaining bars.

Fig. 1

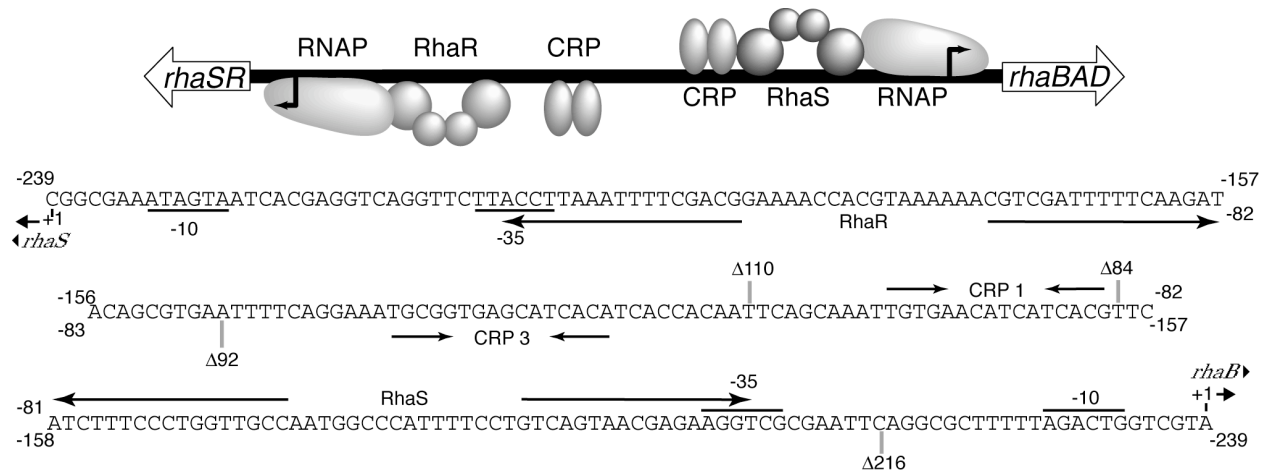
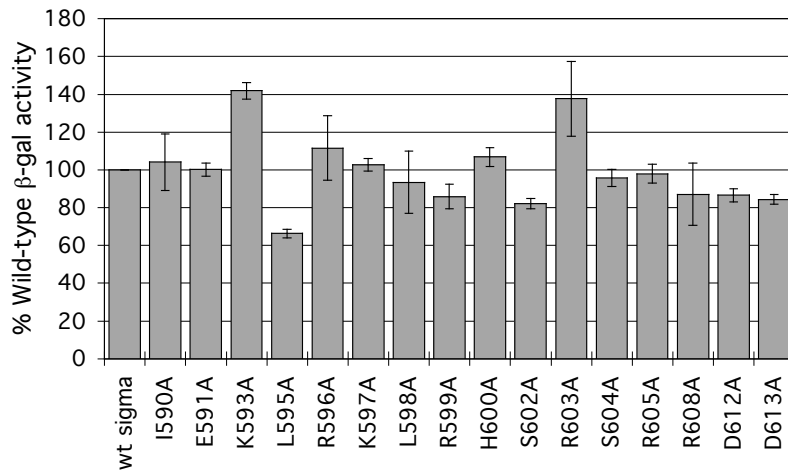


Fig. 2

A. $\Delta(rhaS-lacZ)\Delta 216$



B. $\Delta(rhaS-lacZ)\Delta 92$

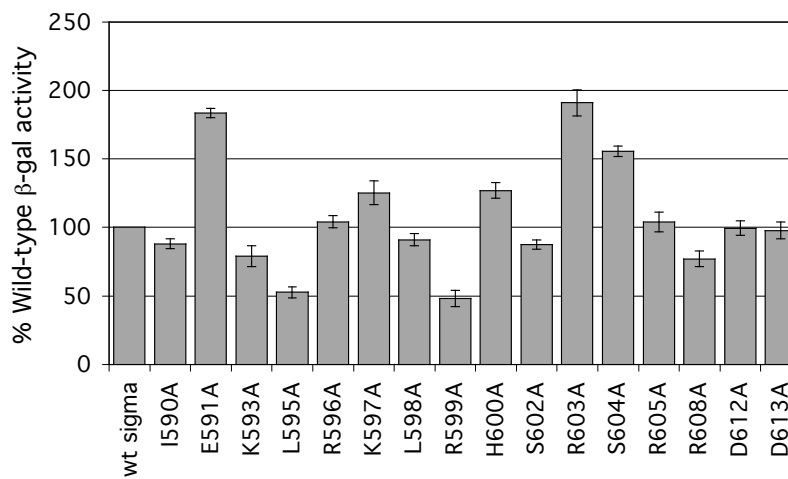


Fig. 3

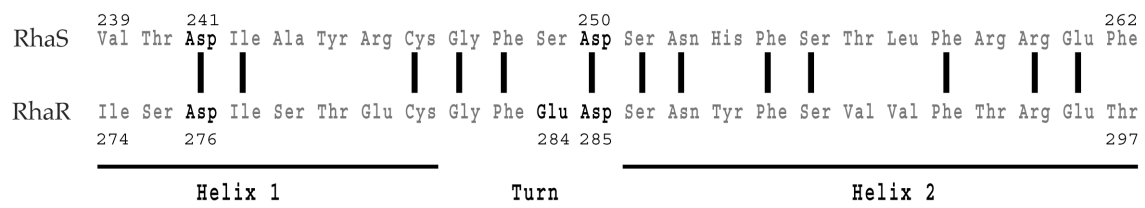


Fig. 4

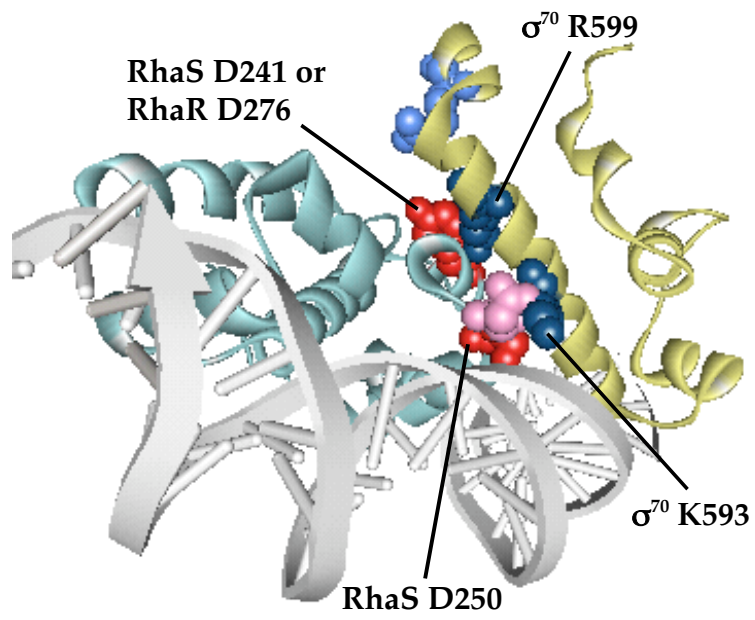


Fig. 5

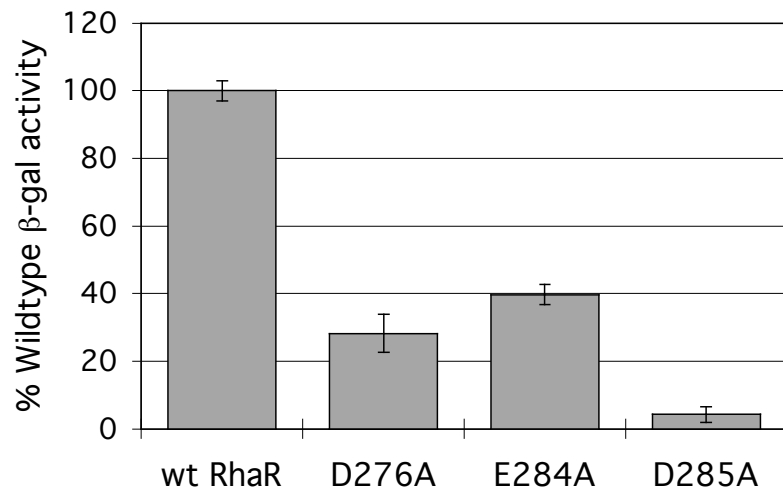
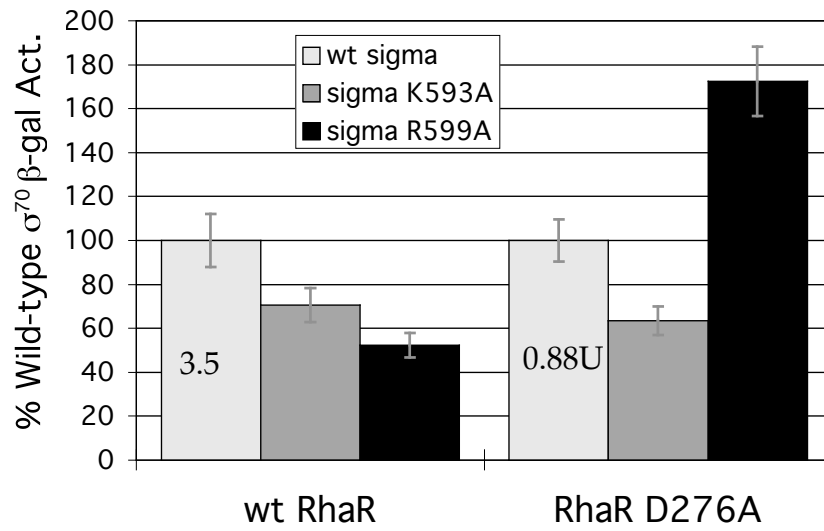


Fig. 6

A.



B.

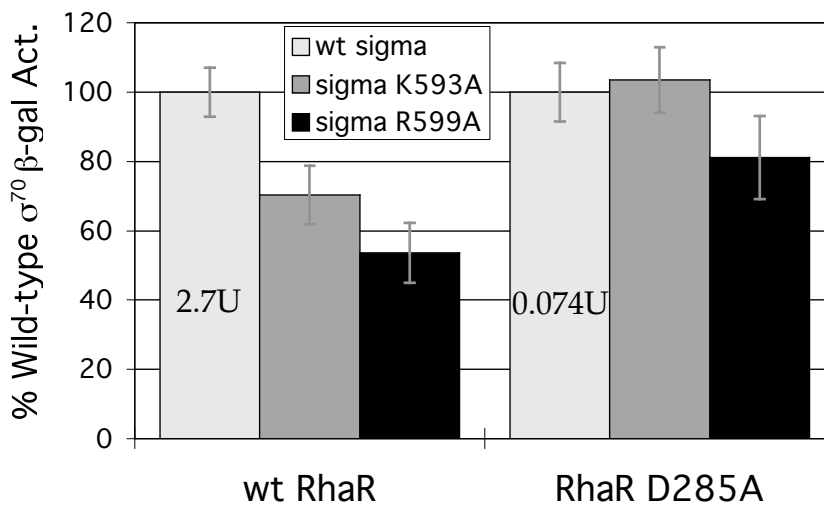
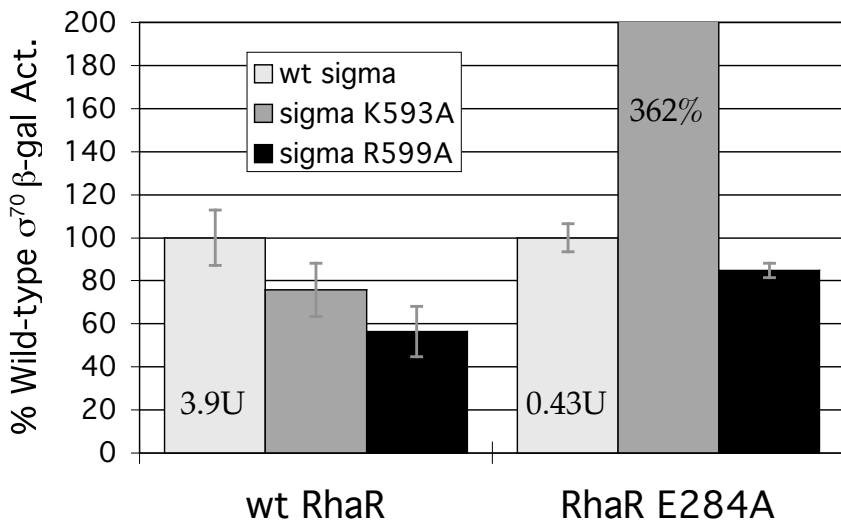


Fig. 6 (continued)

C.



D.

